Catalytic Activity and Inhibition of Human Histone Deacetylase 8 Is Dependent on the Identity of the Active Site Metal Ion†

Stephanie L. Gantt,‡ Samuel G. Gattis,§ and Carol A. Fierke*,‡,§

Departments of Chemistry and Biological Chemistry, University of Michigan, 930 North University Avenue, Ann Arbor, Michigan 48109-1055

Received February 1, 2006; Revised Manuscript Received March 13, 2006

ABSTRACT: Histone deacetylases play a key role in regulating transcription and other cellular processes by catalyzing the hydrolysis of ϵ-acetyl-lysine residues. For this reason, inhibitors of histone deacetylases are potential targets for the treatment of cancer. A subset of these enzymes has previously been shown to require divalent metal ions for catalysis. Here we demonstrate that histone deacetylase 8 (HDAC8) is catalytically active with a number of divalent metal ions in a 1:1 stoichiometry with the following order of specific activity: Co(II) > Fe(II) > Zn(II) > Ni(II). The identity of the catalytic metal ion influences both the affinity of the HDAC inhibitor suberoylanilide hydroxamic acid (SAHA) and the Michaelis constant, with Fe(II)- and Co(II)-HDAC8 having K_M values that are over 5-fold lower than that of Zn(II)-HDAC8. These data suggest that Fe(II), rather than Zn(II), may be the in vivo catalytic metal. In further support of this hypothesis, recombinant HDAC8 purified from *E. coli* contains 8-fold more iron than zinc before dialysis, and the HDAC8 activity in cell lysates is oxygen-sensitive. Identification of the in vivo metal ion of HDAC8 is essential for understanding the biological function and regulation of HDAC8 and for the development of improved inhibitors of this class of enzymes.

Post-translational modification of histones is important for the regulation of gene expression. These covalent modifications include phosphorylation, methylation, ubiquitylation, sumoylation, and acetylation (*1*, *2*). Many nonhistone transcription factors and other proteins are also acetylated (*3*) with the balance between acetylated and nonacetylated proteins controlled by the activity of histone acetyltransferases (HATs[1]) and histone deacetylases (HDACs), respectively (Scheme 1). Decreased histone acetylation silences affected genes and has been linked to cancer development (*4*). Inhibitors of HDACs increase histone acetylation; in malignant cells, these inhibitors reactivate the expression of dormant $p21^{WAF1}$ and are showing promise in clinical trials for cancer treatment, with relatively few side effects because of the selective targeting of cancer cells (*5*−*7*).

Scheme 1: Balance between Acetylated and Nonacetylated Lysine Residues Is Controlled by Histone Deacetylase (HDAC) and Histone Acetyltransferase (HAT) Activities

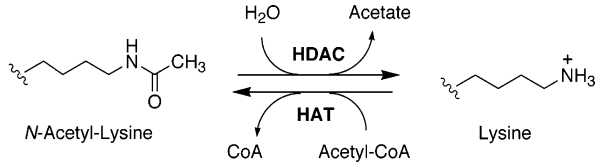

There are 18 known human HDACs, which are divided into three groups on the basis of sequence similarity. HDACs in classes I (HDAC1−3, 8, and 11) and II (HDAC4−7, 9, and 10) are metalloenzymes with a largely conserved catalytic core, consistent with a common catalytic mechanism (*8*). Class II HDACs are distinguished by added sequence extensions not found in class I (*9*). Most HDAC inhibitors target these two classes of enzymes (*10*). Class III HDACs require NAD^+ as a cosubstrate, share no sequence similarity with class I and II HDACs, and use an alternative catalytic mechanism (*11*).

HDAC8 is a member of the class I histone deacetylases and has been shown by immunochemistry to localize mainly with the cytoskeleton of smooth muscle cells (*12*). HDAC8 activity decreases when phosphorylated by protein kinase A, in contrast to HDAC1 and HDAC2, which are activated by phosphorylation (*13*). Oxidative stress also causes a decrease in overall HDAC catalytic activity (*14*) through an unidentified mechanism. HDAC8 has been validated as a cancer target by the elevated levels of HDAC8 mRNA in some cancer cells (*15*) and by the antiproliferative effect of RNA interference directed toward HDAC8 (*16*).

† This work was supported by National Institutes of Health Grant GM40602 (C.A.F.). S.L.G. was supported in part by a NSF predoctoral fellowship and by the NIH Chemistry-Biology Interface Training Program (T32 GM08597). S.G.G. was supported in part by the NIH Pharmacological Sciences Training Program (T32 GM07767). The contents of this publication are solely the responsibility of the authors and do not necessarily represent the official views of NIGMS.

* To whom correspondence should be addressed. Tel: (734) 936-2678. Fax: (734) 647-4865. E-mail: fierke@umich.edu.

‡ Department of Chemistry.

§ Department of Biological Chemistry.

[1] Abbreviations: EDTA, ethylenediaminetetraacetic acid; GABC, general acid/base catalysis; HAT, histone acetyltransferase; HDAC, histone deacetylase; HDLP, histone deacetylase-like protein; ICP-MS, inductively coupled plasma-mass spectrometry; LpxC, UDP-3-*O*-acyl-*N*-acetylglucosamine deacetylase; MOPS, 4-morpholinepropanesulfonic acid; Ni-IMAC, Ni(II)-immobilized metal affinity chromatography; PMSF, phenylmethylsulfonyl fluoride; SAHA, suberoylanilide hydroxamic acid; TAME, tosyl-arginine methyl ester; TCEP, tris(2-carboxyethyl) phosphine; TSA, trichostatin A.

10.1021/bi060212u CCC: $33.50
Published on Web 04/25/2006

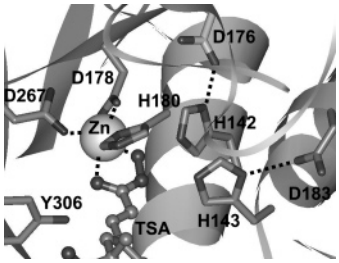

FIGURE 1: Active site of HDAC8 with a bound TSA hydroxamate inhibitor. D178, H180, D267, and TSA are direct metal ligands. H142 and H143 are the proposed general base and general acid catalysts, with hydrogen bonds to D176 and D183, respectively. (From pdb # 1T64 (*20*).)

A chemical mechanism has been proposed for the metal-dependent HDACs (*17*), on the basis of biochemical and genetic data (*18*, *19*) as well as the crystal structures of HDAC8 and a bacterial histone deacetylase-like protein (HDLP) (*16*, *17*, *20*). In this mechanism, the catalytic metal ion and a general base (H142) activate the water molecule for nucleophilic attack on the substrate carbonyl (Figure 1). The tetrahedral intermediate is stabilized by the formation of a hydrogen bond with Y306, and a general acid (H143) protonates the lysine leaving group to catalyze the formation of the products from the tetrahedral intermediate. Both H142 and H143 are part of His-Asp dyads, which are proposed to modulate the basicity of the His residues (*17*). The use of two histidines as a general acid/base catalytic (GABC) pair is unlike the prototypical metalloprotease mechanism that uses a single GABC (*21*). However, a GABC pair mechanism has been proposed for other metal-dependent deacetylases, including UDP-3-*O*-acyl-*N*-acetylglucosamine deacetylase (LpxC) (*21*, *22*). Although the available data support this mechanism, it has yet to be biochemically shown for any class I or II HDACs.

The metal-dependent HDACs have been designated as zinc-dependent enzymes (*10*) because the addition of Zn(II) increases HDLP activity, and a Zn(II) ion was observed in the active site of the HDLP crystal structure with the bound hydroxamate inhibitor trichostatin A (TSA) (*17*). Interestingly, the HDACs possess an unusual set of metal ligands for a mononuclear Zn(II) enzyme (*23*), Asp_2-His-water, suggesting that Zn(II) may not be the in vivo metal ion. Other members of the histone deacetylase superfamily, the acetylpolyamine amidohydrolases, are activated by Zn(II) and Co(II) (*24*, *25*). The HDACs are also inhibited by millimolar Zn(II) (*26*−*28*), suggesting the presence of a second metal binding site. Furthermore, the observation of a single metal ion in the HDAC8 and HDLP crystal structures is not conclusive evidence that HDACs are mononuclear enzymes because the second metal of binuclear enzymes does not always bind tightly enough to be resolved in crystal structures, as observed for metallo-β-lactamase (*29*). HDAC8 and HDLP are structurally homologous to the di-manganese enzyme arginase (*30*), leading to the proposal that HDACs could be binuclear enzymes (*17*). These findings suggest that HDACs could potentially bind more than one metal ion and/or be activated by metal ions other than zinc.

In this work, we demonstrate that HDAC8 is maximally active with a single bound metal ion. The highest catalytic activity is observed for a 1:1 complex of HDAC8 with Co(II), although HDAC8 is also activated by the stoichiometric addition of other metal ions in the order Co(II) > Fe(II) > Zn(II) > Ni(II). These data raise the possibility that HDAC8 may function as an Fe(II) metalloenzyme in vivo, as recently suggested for a number of other enzymes originally proposed to be Zn(II) enzymes (*31*−*33*). The identity of the HDAC8 active site metal ion is important because it affects the catalytic activity and the apparent substrate and inhibitor affinities. Furthermore, it is possible that HDAC8 is regulated under oxidative stress conditions by changes in the oxidation state or the identity of the catalytic metal ion.

EXPERIMENTAL PROCEDURES

Materials. Unless otherwise specified, chemicals and supplies were purchased from Fisher. Ethylenediaminetetraacetic acid (EDTA) and $FeCl_2$ were purchased from Aldrich and chromatography resins from GE Healthsciences. All chemicals were of the highest quality available. His_6-tagged TEV NIa protease was recombinantly expressed from pET-20d-TEV NIa, a generous gift from Dr. Z. Xu (University of Michigan), and purified as described (*34*). Suberoylanilide hydroxamic acid (SAHA) was synthesized according to published procedures (*35*).

Plasmid Construction. The pET-20b-derived HDAC8 *E. coli* expression plasmid, pHD2-His (Gantt, S. L. and Fierke, C. A., unpublished data), was modified to add a TEV NIa protease cleavage site with the linker recommended by Invitrogen (ENLYFQ|G-DYDIPTT) upstream of the *C*-terminal His_6 tag. After cleavage, this construct adds six amino acids (-ENLYFQ) to the *C*-terminus of HDAC8, whereas the sequence of the *N*-terminus is identical to that of the native protein (*34*). An insert including the TEV recognition sequence flanked by *Stu* I and *Xho* I restriction sites was created using a primer overlap extension (*36*) and then amplified using the polymerase chain reaction (primer 1: 5′-GCC AAG CTG C***AG GCC T***GA CCG CAA CGA GCC GCA CCG CAT CCA GCA GAT CCT CAA CTA CAT CAA AGG CAA CCT GAA ACA C-3′ and primer 2: 5′-GGT CGA CCT G***CT CGA G***GG TGG TCG GGA TGT CGT AGT CAC CCT GGA AGT ACA GGT TCT TAA CAA CGT GTT TCA GGT TGC CTT TGA TG-3′). A *Stu* I site was introduced into pHD2-His at Arg353 using the QuikChange mutagenesis kit (Stratagene). This plasmid and the PCR fragment were each digested with *Stu* I and *Xho* I, purified using an agarose gel, and then joined by reaction with T4 DNA ligase (New England Biolabs) to create pHD2-TEV-His. The plasmid sequence was verified by the University of Michigan DNA sequencing core.

HDAC8-His Expression. BL21(*DE3*)pHD2-TEV-His cells were grown in 2X−YT media at 37 °C and induced by the addition of isopropyl-β-D-thiogalactoside (0.4 mM) and $ZnSO_4$ (0.2 mM) when $A_{600} = 0.7-0.8$. The temperature was decreased to 25 °C at induction, and protease inhibitors (10 μg/mL of phenylmethylsulfonyl fluoride (PMSF) and 1 μg/mL of tosyl-arginine methyl ester (TAME)) were added 3.5 h after induction. The cells were incubated at 25 °C for an additional 14 h and harvested by centrifugation (6000*g*, 15 min, 4 °C). The cells were resuspended in buffer A (30 mM Hepes, pH 8.0, 0.5 mM imidazole and 150 mM NaCl) with 10 μg/mL of PMSF and 1 μg/mL of TAME and frozen at −80 °C.

HDAC8 Purification. The cells were lysed using a microfluidizer (Microfluidics) and centrifuged at 45 000*g* for

1 h. The cleared lysate was bound to a $NiSO_4$-charged immobilized metal affinity column (Ni-IMAC) and then eluted with a step gradient of increasing imidazole concentration (0.5, 25, 50, 100, and 200 mM imidazole in 30 mM Hepes at pH 8.0 and 150 mM NaCl). His_6-tagged TEV NIa protease was added (0.1 mg/mL) to the fraction containing HDAC8-His, and the reaction was dialyzed overnight at 4 °C against buffer A with 1 mM tris(2-carboxyethyl) phosphine (TCEP). The cleaved HDAC8 was purified on a second Ni-IMAC column. HDAC8 was eluted with 25 mM imidazole, whereas HDAC8-His and His_6-tagged TEV NIa protease were eluted with 200 mM imidazole. HDAC8 was dialyzed overnight at 4 °C against 10 mM Hepes at pH 7.5, 100 mM NaCl, and 1 mM TCEP, concentrated to 200−500 μM, and stored at −80 °C. The concentration of HDAC8 was determined by measuring the A_{280} value under denaturing conditions using a calculated ϵ_{280} value of 52 120 $M^{-1}cm^{-1}$ (*37*); similar concentrations of HDAC8 were obtained with the bicinchoninic acid assay (*38*) using bovine serum albumin as a protein standard. The purity of the final HDAC8, determined by SDS−PAGE, was ≥95%. The catalytic activity of HDAC8-His was not changed by the removal of the His_6-tag (data not shown). The metal content of HDAC8 was measured by inductively coupled plasma-mass spectrometry (ICP-MS) using a facility in the Geology Department at the University of Michigan.

Metal-Free HDAC8 Preparation. All plasticware and syringes used to make metal-free HDAC8 were soaked in 1 mM EDTA overnight and extensively washed with Milli-Q ddH_2O. Low-metal pipet tips and plastic vials were used for all experiments involving apo-HDAC8. To prepare the apo enzyme, HDAC8 (100 μM) was dialyzed overnight against two exchanges of 25 mM 4-morpholinepropanesulfonic acid (MOPS) at pH 7.0, 1 mM EDTA, and 10 μM dipicolinic acid at 4 °C, followed by dialysis against 25 mM MOPS at pH 7.5 and 0.1 mM EDTA. The calculated concentration of EDTA in the apo-HDAC8 was reduced to less than 2 μM by buffer exchange with a Microcon centrifugal filtration device (10 000 MWCO, Millipore) using buffer C (25 mM MOPS at pH 7.5 and 1 μM EDTA), followed by a PD-10 gel filtration column equilibrated with buffer C. Apo-HDAC8 was concentrated to 100−200 μM, flash-frozen and stored at −80 °C. HDAC8 contains 10 Cys residues, which were used to verify the concentration of apo-HDAC8 using the Ellman assay (*39*).

HDAC8 Activity Assay. The catalytic activity of HDAC8 was measured using the commercially available Fluor de Lys HDAC8 peptide substrate (R-H-K(Ac)-K(Ac)-fluorophore) (BIOMOL), which is based on the sequence of acetylated p53. The basis of this assay is a shift in the wavelength and intensity of fluorescence upon proteolytic cleavage of the peptide following deacetylation of the *C*-terminal substrate lysine. This is monitored by measuring the fluorescence of both the deacetylated product (ex = 340 nm, em = 450 nm) and the remaining substrate (ex = 340 nm, em = 380 nm), following the incubation of quenched reactions with the protease developer. The metal was bound to the enzyme by the incubation of apo-HDAC8 (2 μM) with atomic absorption metal standard on ice for 1 h prior to dilution into the assay mix; the addition of metal does not affect the pH. Except where noted, the assays contained 50 μM substrate and 0.4 μM HDAC8 at 25 °C in the assay buffer (25 mM Tris at pH 8.0, 137 mM NaCl, and 2.7 mM KCl), which was treated with Chelex resin (Bio-Rad) to remove trace divalent metal ions. Aliquots were quenched by dilution into 1 μM TSA (a HDAC inhibitor) and Fluor de Lys Developer II (BIOMOL). The fluorescence from both product and substrate were measured using a fluorescence plate reader (BMG Labtech). The ratio of the product fluorescence divided by the substrate fluorescence increases with product concentration and is linear up to 30% product. The concentration of the product at each time point was calculated from a standard curve prepared by using solutions containing known concentrations of the product (0−10 μM) with the total concentration of the product and substrate maintained at 50 μM and then diluted into quench. The product was formed by reacting the substrate to completion and quenching the reaction with 10 μM TSA and Developer II. ICP-MS data demonstrate that concentrations of Fe, Ni, Mn, Co, and Cu in the assay buffer and substrate are below the 0.01 μM detection limit of the instrument. The Fluor de Lys HDAC8 substrate contains a small concentration of Zn (0.01−1.0 μM per 50 μM substrate), which varies by lot number. Only the substrate lots containing less than 0.03 μM Zn per 50 μM substrate were used for the metal-dependent measurements.

The kinetic parameters k_{cat}, k_{cat}/K_M and K_M for Co(II)-, Fe(II)-, and Zn(II)-HDAC8 were determined by fitting the Michaelis−Menten equation to the initial velocity as a function of substrate concentration for 1.2 μM metal-substituted HDAC8. The values of k_{cat}/K_M for Fe(III)-, Mn(II)-, Ni(II)-, and apo-HDAC8 were determined by dividing the initial rate for deacetylation by the concentration of the enzyme (0.4 μM) and subsaturating substrate (50 μM).

The SAHA inhibition constant (K_i) for metal-substituted HDAC8 was determined by globally fitting eq 1 using Prism 4.0 (GraphPad Software, Inc.) to the initial velocity for enzyme assays, varying the concentrations of both enzyme (E_{tot}, 0.2−0.8 μM) and SAHA (I_{tot}, 0−3 μM) at 50 μM substrate. At $[S] \ll K_M$, the K_{app} value is nearly equal to the inhibition constant K_i.

$$\frac{v}{v_0} = \frac{E_{tot} - I_{tot} - K_{app} + \sqrt{(E_{tot} - I_{tot} - K_{app})^2 + 4E_{tot}K_{app}}}{2E_{tot}} \quad \text{(eq 1)}$$

All work with Fe(II) was performed anaerobically in a N_2/H_2 atmosphere glovebox from Coy Labs. The dissolved oxygen was removed from ddH_2O by sparging with argon and incubating for 24 h in the glovebox. $FeCl_2$ was dissolved in anaerobic ddH_2O and used within 1 h. The enzyme and substrate (<10 μL) were each allowed to equilibrate in the glovebox for at least 2 h at 4 °C before Fe(II) was added; Fe(II) was incubated with apo-HDAC8 for 15 min prior to beginning the assays.

To test for the incorporation of iron into HDAC8 during cell growth, ferric citrate (1 mg/mL), rather than zinc, was added to the cell culture at induction. The pelleted cells were frozen under argon and then lysed and assayed for HDAC8 activity either anaerobically (in the glovebox) or aerobically. The cells were lysed by treatment with B-Per II cell lysis solution (Pierce) and incubated at 4 °C for 25 min. The cell

Table 1: Metal Content of Purified HDAC8[a]

metal	initially purified HDAC8-His[b]	HDAC8[c]	apo-HDAC8[d]
Fe	0.8	0.03[f,g]	0.02[e,g]
Ni	0.5	0.2[f,h]	0.01[e,i]
Zn	0.1	1.0[f,g]	0.03[f,g]
Co	<0.001	<0.007	<0.002
Cu	0.01	0.02[f,h]	0.01[e,g]
Mn	0.004	<0.002	<0.003
total	1.4	1.3[f,g]	0.07[f,h]

[a] The average metal content is expressed as mol metal/mol HDAC8. [b] The metal content measured in one preparation of HDAC8-His after the first Ni-IMAC column without dialyzing or concentrating the protein. [c] The metal content in HDAC8 after all of the purification steps; an average of three preps. [d] An average of four preps, two of which used the HDAC8-TEV purified using slightly different conditions but with the same protocol for removing metal. [e] The range of measured metal concentrations had lower limits of 4−20% of the average. [f] The range of measured metal concentrations had lower limits of 30−70%. [g] The range of measured metal concentrations had upper limits of 110−170% of the average. [h] The range of measured metal concentrations had upper limits of 200−250%. [i] The range of measured metal concentrations had upper limits of 400%.

debris was then pelleted, and the cleared lysate was assayed for catalytic activity using 100 μM Fluor de Lys HDAC8 substrate in standard assay buffer.

RESULTS

Preparation of Recombinant HDAC8. HDAC8-His was recombinantly expressed in *E. coli* and purified aerobically using a Ni-IMAC column. At this point, the metal content of the fraction containing the highest concentration of >90% pure HDAC8-His protein was determined by ICP-MS. This HDAC8-His fraction contains a significant amount of iron and nickel, with a metal to enzyme stoichiometry of 0.8 Fe, 0.5 Ni, and 0.1 Zn (Table 1). To avoid complications caused by metal ions binding to the His_6-tag, the tag was then cleaved from HDAC8-His, followed by a final Ni-IMAC column to yield >95% pure HDAC8. After dialysis of HDAC8 against buffers containing no added metals and under aerobic conditions, the ratio of bound metal to HDAC8 from multiple enzyme preparations was determined. The most abundant metal present in this HDAC8 is Zn, with a metal to enzyme stoichiometry ranging from 0.5 to 1.4; this is likely acquired during dialysis from low levels of contaminating zinc in the buffers and the dialysis tubing. (Buffers can contain 0.02−0.15 μM Zn unless they have been treated with Chelex or care is taken to ensure that zinc is not acquired during the buffer preparation or storage.) Significant amounts of Ni are also present in the purified HDAC8; presumably, the Ni content is elevated because of purification using the Ni-IMAC column. A significant decrease in the bound iron concentration is observed following dialysis, indicating an exchange with zinc. Dialysis of HDAC8 against chelators yields apo-HDAC8 containing 0.03−0.15 total bound mol metal ion/mol enzyme; apo-HDAC8 containing ≤0.08 metal/enzyme was used for all assays.

One Catalytic Metal Ion/HDAC8. The apo-HDAC8 was reconstituted with divalent metal ions prior to activity measurements. The initial velocity for the catalysis of deacetylation of the Fluor de Lys HDAC8 substrate is linearly dependent on both the concentration of the substrate and HDAC8. Apo-HDAC8 consistently displays a residual level of catalytic activity (~7% of the Zn-HDAC8 rate, Table 2), which is likely due to the small amounts of metal contamination in both the substrate and the apo enzyme (Table 1). It is also possible, although unlikely, that apo-HDAC8 retains some catalytic activity.

To assess whether the catalytically active form of HDAC8 contains a mononuclear or binuclear metal site, the observed steady-state velocity was measured as a function of metal ion stoichiometry. Several divalent metal ions were evaluated for the ability to activate HDAC8. No activation of catalytic activity is seen after the incubation of apo-HDAC8 with 0.5, 1, or 2 mol of Fe(III) or Mn(II) per mol of HDAC8. In contrast, for Co(II)-, Fe(II)-, or Zn(II)-HDAC8, the activity increases linearly with increasing metal ion concentration until a stoichiometry of 1 mol metal/mole HDAC8 is reached, at which point no further increase in activity is observed (Figure 2). These data clearly indicate that HDAC8 requires one catalytic metal ion for maximal activity and that a variety of divalent metal ions can activate HDAC8 activity. The linear dependence of activity on metal ion concentration indicates that the K_D value for the dissociation of Co(II), Fe(II), or Zn(II) from the HDAC8−metal complex is lower than the micromolar concentration of enzyme in the assay; the affinity of catalytic Zn(II) and Fe(II) metal sites is typically in the pM to nM range (*40*, *41*). The activation of HDAC8 by Ni(II) could be described by either stoichiometric binding or a single binding isotherm (K_D ~ 200 nM). The activity of Fe(II)-HDAC8 was measured under anaerobic conditions to prevent the oxidation of Fe(II) to Fe(III). The exposure of Fe(II)-substituted HDAC8 to air for 2 min causes the catalytic activity to decrease by >85%, suggesting that Fe(II) bound to HDAC8 is readily oxidized to Fe(III) upon exposure to oxygen. These data clearly indicate that HDAC8 requires one catalytic metal ion for maximal activity and that a variety of divalent metal ions can activate HDAC8 activity.

Metal Inhibition. The addition of a second equivalent of Zn(II) halves the HDAC8 activity (Figure 2), indicating that a second zinc ion binds to an inhibitory site in HDAC8, as observed for other metalloenzymes (*21*, *42*, *43*). Co(II), Fe(II), and Ni(II) did not significantly inhibit HDAC8 upon addition of 2 equivalents of metal (Figure 2), suggesting that the inhibitory site has a weaker affinity for these metals. Inhibition is observed at higher concentrations of Co(II) and Fe(II) (~20 μM), consistent with this hypothesis. To test whether Fe(III) could inhibit HDAC8, 0.4 μM Zn(II)-HDAC8 was incubated with 0−8 μM Fe(III) for 30 min, and the catalytic activity was measured. HDAC8 activity decreases with added Fe(III), with a K_i value of 0.7 μM (data not shown), indicating that excess Fe(III) inhibits HDAC8. Although this metal inhibits Zn(II)-HDAC8, Fe(III) does not displace Zn(II) bound to HDAC8, but Zn(II) can displace Fe(III) bound to HDAC8 (data not shown). It is not known whether the inactive Fe(III)-HDAC8 (Table 2) contains Fe(III) in the catalytic site or the inhibitory site.

Kinetic Rate Constants of Metal-Substituted HDAC8. HDAC8 was stoichiometrically substituted with transition metals, and the specific activity was measured for the catalysis of deacetylation of the Fluor de Lys HDAC8 substrate. The following trend in k_{cat}/K_M values is observed: Co(II) > Fe(II) > Zn(II) > Ni(II), with no activity over background observed for Fe(III)- or Mn(II)-substituted

Table 2: Reactivity of Metal-Substituted HDAC8[a]

enzyme	k_{cat}/K_M ($M^{-1}s^{-1}$)	k_{cat} (s^{-1})	K_M (μM)	relative rate[b]	SAHA K_i (nM)
Co(II)-HDAC8	7500 ± 300[c]	1.2 ± 0.2[c]	160 ± 6[c]	9.4 ± 0.7	44 ± 15
Fe(II)-HDAC8	2300 ± 160[c]	0.48 ± 0.01[c]	210 ± 20[c]	2.8 ± 0.3	130 ± 40
Zn(II)-HDAC8	800 ± 50[c]	0.90 ± 0.03[c]	1100 ± 50[c]	1.0	250 ± 25
Ni(II)-HDAC8	110 ± 8[d]	n.d.[e]	n.d.	0.14 ± 0.01	n.d.
Mn(II)-HDAC8	40 ± 9[d]	n.d.	n.d.	0.05 ± 0.01	n.d.
Fe(III)-HDAC8	<10[f]	n.d.	n.d.	<0.01	n.d.
apo-HDAC8	60 ± 20[d]	n.d.	n.d.	0.07 ± 0.02	n.d.

[a] The metal-substituted HDAC8 was prepared and assayed as described in the legend of Figure 2. [b] The value of k_{cat}/K_M for each metal-substituted HDAC8 relative to that for Zn(II)-HDAC8. [c] The steady-state kinetic parameters were calculated from a fit of the Michaelis−Menten equation to the dependence of the initial rate on the substrate concentration at 1.2 μM HDAC8. [d] An average of three measurements ± standard deviation at 0.4 μM HDAC8 and 50 μM substrate. [e] The value was not determined. [f] The initial velocity using 0.4 μM Fe(III)-HDAC8 was not detectable.

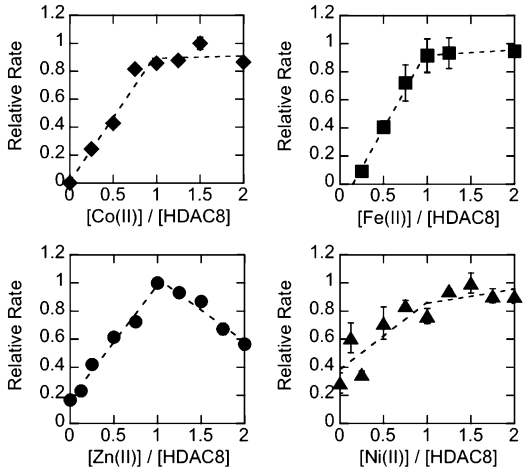

FIGURE 2: Metal stoichiometry. Apo-HDAC8 (2 μM) was incubated with metal (Co(II) (♦), Fe(II) (■), Zn(II) (●), or Ni(II) (▲) at 4 °C for 15 min (Fe(II)) or 1 h (all other metals) and then diluted to 0.4 μM by the addition of the Fluor de Lys HDAC8 substrate (50 μM) at 25 °C in 25 mM Tris at pH 8.0, 140 mM NaCl, and 2.7 mM KCl. The initial rates for deacetylation were determined from time-dependent changes in fluorescence. The observed rates for each metal ion were normalized to the highest rate for a given metal ion. The absolute activity in the absence of added metal ion was the same in each case.

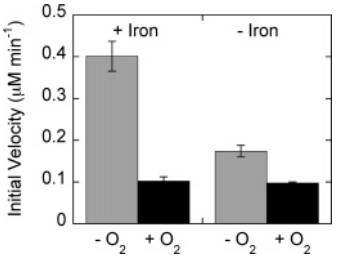

FIGURE 3: HDAC activity of cell lysates. The cells were grown with (+Iron) or without (−Iron) iron supplementation following induction. The cells were lysed and assayed for HDAC activity as described in Experimental Procedures either anaerobically ($-O_2$) or aerobically ($+O_2$). Exposure of cell lysate to air decreases HDAC8 activity in both sets of cells but to a greater extent in cells that were grown with added iron.

HDAC8 (Table 2). Co(II)-HDAC8 and Fe(II)-HDAC8 are 9.4-fold and 2.8-fold, respectively, more active than Zn(II)-HDAC8, whereas Ni(II) activates apo-HDAC8 less than 2-fold. The values of k_{cat}/K_M measured for HDAC8 reconstituted with Fe(II), Co(II), or Zn(II) are significantly higher than those previously reported (44), with Zn(II)-HDAC8 showing a 15-fold larger value of k_{cat}/K_M. This enhancement of activity may be due to the stoichiometric reconstitution with divalent metals and/or differences in the substrate used to assay the activity (Ac-G-A-K(Ac)-7-amino-4-methylcoumarin (44) vs Fluor de Lys HDAC8, which is R-H-K(Ac)-K(Ac)-fluorophore).

The k_{cat} values are less dependent on the identity of the metal ion than k_{cat}/K_M. HDAC8 substituted with Co(II) has the highest value of k_{cat} (1.2 s^{-1}), whereas Zn(II)-HDAC8 (0.90 s^{-1}) has a faster k_{cat} value than Fe(II)-HDAC8 (0.48 s^{-1}) (Table 2). However, the metal identity has a marked effect on K_M; the K_M values of Co(II)-HDAC8 and Fe(II)-HDAC8 are 6.8- and 5.2-fold, respectively, lower than that of Zn(II)-HDAC8 (Table 2).

The high specific activity of Fe(II)-HDAC8 and the high iron content in the initially purified enzyme suggest that HDAC8 recombinantly expressed in *E. coli* may bind Fe(II) as the in vivo metal ion. To examine this possibility further, ferric citrate was added to the cell culture during HDAC8-His expression. This source of iron is slowly absorbed by *E. coli* and can be intracellularly reduced to Fe(II) (*45*). For cells grown with iron supplementation, the HDAC8 activity is ~4-fold larger when the cells are lysed and assayed under anaerobic conditions compared to that under aerobic conditions (Figure 3). This increase in activity is consistent with the ratio of activities of Fe(II)- and Zn(II)-substituted HDAC8s (Table 2), suggesting that the decrease in activity is caused by a switch in the active site metal ion. Alternatively, the decrease in activity could be caused by the formation of Fe(III)-inhibited HDAC8. The lysate from cells grown in nonsupplemented media also shows increased HDAC activity when lysed and assayed anaerobically, although the difference is less pronounced (~2-fold). These data suggest that HDAC8 expressed in *E. coli* incorporates redox-sensitive Fe(II) as the active site metal ion, with the extent of iron incorporation being dependent on the concentration of iron available during growth.

Inhibition by SAHA. Inhibition of HDAC8 by the hydroxamic acid inhibitor SAHA is also dependent on the active site metal ion. Because of the instability of HDAC8 at concentrations below ~0.2 μM (data not shown), the inhibition constant for SAHA was determined as a function of both the enzyme and inhibitor concentrations using eq 1. The measured K_i values follow the same trend as that of k_{cat}/K_M, with Co(II)-HDAC binding SAHA with the highest affinity (44 ± 15 nM), followed by Fe(II)-HDAC8 (130 ± 40 nM) and Zn(II)-HDAC8 (250 ± 25 nM) (Table 2; Figure 4). The decreased affinity of Zn(II)-HDAC8 for SAHA

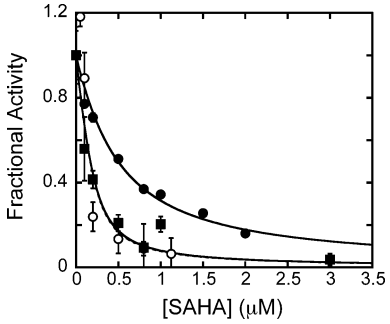

FIGURE 4: Inhibition of HDAC by SAHA. A solution of holo-HDAC8 (Co(II) (○), Fe(II) (■), or Zn(II) (●)) (final concentration of 0.2 μM) was added to a reaction containing 50 μM Fluor de Lys HDAC8 substrate at 25 °C in 25 mM Tris at pH 8.0, 140 mM NaCl, 2.7 mM KCl, and 0−3 μM SAHA. Initial velocities were determined from fluorescence changes over time. Inhibition constants were calculated from a fit of eq 1 to the initial rates of deacetylation for 0−3 μM inhibitor and 0.2−0.8 μM enzyme.

suggests an alteration in the active site environment upon metal substitution.

DISCUSSION

Metal Stoichiometry. Although histone deacetylases have been shown to be metalloenzymes by crystallography (*17*) and biochemical analysis (*19*, *26*, *28*), little is known about the metal ion dependence of HDAC activity. To determine whether HDAC8 requires one or two bound metal ions for catalysis, the metal stoichiometry of apo-HDAC8 activation was measured. These data clearly demonstrate that HDAC8 requires one bound metal ion for maximal activity (Figure 2), which is consistent with the proposed catalytic mechanism. Additionally, excess Zn(II) inhibits HDAC8, explaining earlier studies demonstrating that HDACs are inhibited, rather than activated, by millimolar Zn(II) concentrations (*26*−*28*). Zinc inhibition is common in metallohydrolase enzymes, including carboxypeptidase A and LpxC (*43*, *46*). Crystal structures of carboxypeptidase A and LpxC with 2 bound metal ions demonstrate that the inhibitory metal binds near the catalytic metal and is coordinated by the putative general base and/or the metal-bound water, precluding catalysis (*47*, *48*). Therefore, the binding site in HDAC8 for inhibitory metals is likely formed by a combination of the side chains of H142, H143, D178, and/or a zinc−water ligand (Figure 1). The crystal structures of HDAC8 show that only a minimal rotation of D178 is required for these three side-chains to optimally orient to coordinate a second metal ion. This inhibitory metal ion binding site could potentially allow the activity of HDACs to be regulated by changes in physiological zinc concentrations, as proposed for the enzymes caspase-3 and glyceraldehyde 3-phosphate dehydrogenase (*49*). Zinc inhibition could be relevant in vivo even if a catalytic metal ion other than zinc is used because the activity of HDAC8 substituted with Co(II) or Fe(II) is also inhibited by added zinc (data not shown).

Metal Specificity. Determining which metal cofactors activate HDAC8 is important for understanding how HDAC8 is regulated and for developing effective HDAC inhibitors. The reaction of HDAC8 with the nonphysiological Fluor de Lys HDAC8 substrate proceeds with relatively low values of k_{cat}/K_M and high K_M values compared to those of the majority of enzymes that react with their physiological

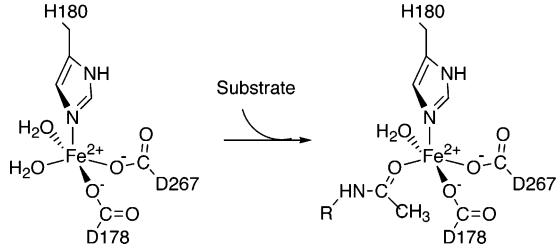

FIGURE 5: Proposed 5-coordinate HDAC8−substrate complex. Binding of the carbonyl oxygen to the metal is predicted to polarize the carbonyl bond, thus activating the carbonyl carbon for nucleophilic attack. A bidentate interaction between the metal and the tetrahedral intermediate could stabilize the transition state for the formation of this intermediate.

substrates near the diffusion-controlled limit (*50*). Thus, it is reasonable to assume that K_M equals K_D^S, reflecting the affinity of the HDAC8 substrate, whereas k_{cat} is the rate constant for the hydrolytic step, although this has not yet been directly demonstrated. Thus far, the only known HDAC8 substrates are the core histones (*26*, *51*, *52*). Other acetylated nonhistone proteins may also be HDAC8 substrates, and the identification of additional substrates remains an area of active research. The steady-state kinetic parameters and the dependence of HDAC8 activity upon stoichiometric metal substitution have yet to be evaluated with full-length protein substrates, which could reasonably be expected to react with lower K_M values than that of the fluorescent tetrapeptide substrate used in the present study.

Measurements of the specific activity of metal-substituted HDAC8 show that Co(II)-substituted HDAC8 is the most active, followed by Fe(II), then Zn(II), and Ni(II) (Table 2). Similar metal dependence was seen with a peptide substrate based on the sequence of histone H4, Fluor de Lys H4-AcK16 (K-G-G-A-K(Ac)-fluorphore) (data not shown). Insight into the HDAC8 catalytic mechanism may be derived from the varying abilities of different metal ions to activate this enzyme. The preference for Co(II) or Fe(II) could be based in part on the need for a catalytic metal ion that can be coordinated by five or six ligands in the transition state and/or that can directly bind and polarize the substrate carbonyl in addition to the catalytic water (Figure 5). A pentacoordinate metal site is supported by the crystal structures of HDAC8, which show that the hydroxamate-inhibited metal site has a distorted square pyramidal metal geometry with H180 as the axial ligand (Figure 1) (*20*). Although catalytic Zn(II) sites can have four to six ligands with a variety of geometries (*21*), the ligand−field stabilization energy of Co(II) and Fe(II) gives these metals a preference for higher coordination numbers (*53*), which may enable Co(II) and Fe(II) to more readily stabilize a 5-coordinate intermediate. The increased affinity of the inhibitor SAHA for Fe(II)- and Co(II)-HDAC8 (Figure 4) is also consistent with a more stable formation of a 5-coordinate species. The crystal structure of SAHA bound to HDAC8 shows that the inhibitor hydroxamate binds to the catalytic metal ion in a bidentate manner (*20*). The lower Michaelis constants observed for Co(II)- and Fe(II)-HDAC8s relative to that for Zn(II)-HDAC8 (Table 2) are consistent with a stronger interaction of the substrate carbonyl with Co(II) or Fe(II) than with Zn(II).

Physiological Metal Ion. The identity of the metal cofactor that activates a given enzyme in vivo is important for

determining how the enzyme is regulated and for developing effective inhibitors; however, the in vivo metal can be difficult to distinguish. Our activity data indicate that the most likely candidates for the metal cofactor used by HDAC8 are Co(II), Fe(II), and Zn(II). It is unlikely that Co(II)-HDAC8 is the physiologically relevant species, despite its higher catalytic activity, because Co(II)-dependent enzymes are extremely rare, with the exception of cobalamin-containing enzymes, and the intracellular cobalt concentration is low (*54*). Of the remaining candidates, Fe(II)-HDAC8 has a higher value of k_{cat}/K_M than Zn(II)-HDAC8. The use of a single catalytic Fe(II) ion has been shown for multiple metallohydrolases, including peptide deformylase, methionyl aminopeptidase, LuxS, γ-carbonic anhydrase, cytosine deaminase, and atrazine chlorohydrolase (*31*−*33*, *55*−*57*). A number of these enzymes were initially misidentified as Zn-metalloenzymes because of the difficulty in measuring Fe(II)-dependent activity and the complications of metal exchange upon oxidation of the active site Fe(II) (*32*, *33*). The trend in specific activity of HDAC8 substituted with Co(II), Fe(II), or Zn(II) parallels that of methionyl aminopeptidase, which is currently proposed to be an Fe(II)-enzyme (*55*). The extent of activation of k_{cat}/K_M for Fe(II) relative to that of Zn(II) in Fe(II)-dependent enzymes such as γ-carbonic anhydrase and peptide deformylase ranges from 1.7- to 100-fold (*31*, *33*). HDAC8 has a 2.8-fold higher k_{cat}/K_M value for Fe(II) than Zn(II), which falls within this range. Other data supporting the use of Fe(II) as the physiological metal by HDAC8 expressed in *E. coli* include the lower substrate K_M value of Fe(II)- relative to that of Zn(II)-HDAC8 (Table 2) and the oxygen sensitivity of the recombinant HDAC8 activity in *E. coli* extracts (Figure 3). Additionally, iron is the most abundant metal in HDAC8-His, immediately following the metal affinity column (Table 1); the bound nickel is likely derived from the metal affinity column. In bacteria and in mammalian cells, where HDAC8 is naturally expressed, the concentration of labile iron is estimated to be orders of magnitude greater than that of labile zinc (nM to μM vs fM to pM), and this intracellular iron is primarily present as Fe(II) (*58*−*61*). Assuming that the identity of the catalytic metal bound to HDAC8 is under thermodynamic control, these results suggest that HDAC8 may use Fe(II) as a metal cofactor in vivo rather than Zn(II). Alternatively, certain metals, including copper, manganese, and iron, can be delivered to their target proteins by metal chaperones (*62*, *63*). If HDAC8 requires a chaperone for metal ion insertion or if the metal identity is controlled by a combination of these two mechanisms, determining the identity of the HDAC8 catalytic metal ion may be more complicated. The metal used could potentially vary by tissue or by HDAC isoform, depending on the specificity of the metal chaperones present, the relative available metal ion concentrations, and/or subtle differences in the exact architecture of each HDAC's metal ion binding site. Knowing the correct physiological metal is crucial because metal substitution alters both substrate and inhibitor affinities in HDAC8 (Table 2 and Figure 4). Inhibitor screens using Zn(II)-HDACs could be systematically underestimating the affinity of candidate compounds; inhibitors in clinical trials, such as SAHA (*64*), may actually be more potent than predicted by in vitro studies using Zn(II). Metal-dependent changes in the affinity and specificity of inhibitors have previously been reported for methionyl aminopeptidase (*65*).

Redox Regulation of HDAC8 Activity. If HDAC8 uses Fe(II) as a metal cofactor in vivo, the oxidation of the catalytic metal ion offers a novel explanation of the previously observed partial inactivation of HDACs by oxidative stress (*14*). The catalytic Fe(II) could be oxidized to Fe(III), which either remains bound as an inactive cofactor in the catalytic or inhibitory site, or the Fe(III) could be displaced by a less active but redox-stable metal such as Zn(II). For instance, calcineurin is regulated by direct oxidation of a catalytic Fe(II) ion to Fe(III) under physiological conditions (*66*). Our data show that HDAC8 can switch from the iron-bound form to the zinc-bound form in vitro; partially purified HDAC8-His initially has high levels of bound iron, which exchange with zinc ions during aerobic dialysis. On the basis of the ratio of k_{cat}/K_M values for Fe(II) and Zn(II)-HDAC8, switching from bound Fe(II) to Zn(II) should cause a 2- to 3-fold loss in HDAC activity under oxidizing conditions. This change in the active site metal ion could potentially alter substrate selectivity as well. Upon treatment of cells with hydrogen peroxide, a 2-fold decrease in HDAC activity has been observed (*67*), which is consistent with either metal switching or the oxidation of a portion of the Fe(II)-HDAC to Fe(III)-HDAC. It is interesting to note that the class III HDACs are also proposed to be regulated by the cellular redox state via changes in the ratio of NAD^+ to NADH (*68*). Metal switching could also be caused by differences in the relative available concentrations of Fe(II) and Zn(II) due to other cellular conditions or to the tissue in which a given HDAC isoform is expressed. Such a mechanism, in which the enzyme has evolved to bind either metal, could explain the reproducible observation of a mixture of metal ions bound to recombinant HDAC8. Because the catalytic activity and Michaelis constant for HDAC8 depend on the catalytic metal ion, in vivo changes in the HDAC8 metal identity or oxidation state may be an important regulatory process.

Summary. We have demonstrated that HDAC8 is a mononuclear metalloenzyme that may use Fe(II) as a metal cofactor in vivo. This is the first time that a metal-dependent HDAC has been shown to be activated by Fe(II). If HDAC8 utilizes Fe(II) under physiological conditions, changes in the cellular redox potential may be an additional way of regulating its activity, although this remains to be tested. Furthermore, altering the identity of the catalytic metal ion between Zn(II) and Fe(II) as a function of cellular conditions may be a novel way of regulating enzyme activity. Consistent with this, the identity of the catalytic metal ion in HDAC8 affects the substrate K_M value and alters the affinity of the inhibitor SAHA. Finally, if Fe(II) is the catalytic metal ion, HDAC inhibitors should be screened in vivo or under anaerobic conditions to prevent the oxidation of the metal cofactor.

ACKNOWLEDGMENT

We thank Dr. Ted Huston for the ICP-MS analysis, Dr. Neil Marsh for use of the anaerobic glovebox, and Dr. Zhaohui Xu for the pET-20d-TEV NIa plasmid. We thank Dr. Dewey McCafferty, Dr. Jennifer Haluko, Dr. David Ballou, and Dr. David Christianson for insightful conversations and members of the Fierke lab for the critical reading of this paper and helpful conversations.

REFERENCES

1. Strahl, B. D., and Allis, C. D. (2000) The language of covalent histone modifications, *Nature 403*, 41−45.
2. Shiio, Y., and Eisenman, R. N. (2003) Histone sumoylation is associated with transcriptional repression, *Proc. Natl. Acad. Sci. U.S.A. 100*, 13225−13230.
3. Yang, X. J. (2004) Lysine acetylation and the bromodomain: a new partnership for signaling, *BioEssays 26*, 1076−1087.
4. Villar-Garea, A., and Esteller, M. (2004) Histone deacetylase inhibitors: understanding a new wave of anticancer agents, *Int. J. Cancer 112*, 171−178.
5. Nebbioso, A., Clarke, N., Voltz, E., Germain, E., Ambrosino, C., Bontempo, P., Alvarez, R., Schiavone, E. M., Ferrara, F., Bresciani, F., Weisz, A., de Lera, A. R., Gronemeyer, H., and Altucci, L. (2005) Tumor-selective action of HDAC inhibitors involves TRAIL induction in acute myeloid leukemia cells, *Nat. Med. 11*, 77−84.
6. Johnstone, R. W., and Licht, J. D. (2003) Histone deacetylase inhibitors in cancer therapy: is transcription the primary target? *Cancer Cell 4*, 13−28.
7. Gui, C. Y., Ngo, L., Xu, W. S., Richon, V. M., and Marks, P. A. (2004) Histone deacetylase (HDAC) inhibitor activation of p21WAF1 involves changes in promoter-associated proteins, including HDAC1, *Proc. Natl. Acad. Sci. U.S.A. 101*, 1241−1246.
8. Khochbin, S., Verdel, A., Lemercier, C., and Seigneurin-Berny, D. (2001) Functional significance of histone deacetylase diversity, *Curr. Opin. Genet. Dev. 11*, 162−166.
9. de Ruijter, A. J., van Gennip, A. H., Caron, H. N., Kemp, S., and van Kuilenburg, A. B. (2003) Histone deacetylases (HDACs): characterization of the classical HDAC family, *Biochem. J. 370*, 737−749.
10. Drummond, D. C., Noble, C. O., Kirpotin, D. B., Guo, Z., Scott, G. K., and Benz, C. C. (2005) Clinical development of histone deacetylase inhibitors as anticancer agents, *Annu. Rev. Pharmacol. Toxicol. 45*, 495−528.
11. Blander, G., and Guarente, L. (2004) The Sir2 family of protein deacetylases. *Annu. Rev. Biochem. 73*, 417-435.
12. Waltregny, D., Glenisson, W., Tran, S. L., North, B. J., Verdin, E., Colige, A., and Castronovo, V. (2005) Histone deacetylase HDAC8 associates with smooth muscle alpha-actin and is essential for smooth muscle cell contractility, *FASEB J. 19*, 966−968.
13. Sengupta, N., and Seto, E. (2004) Regulation of histone deacetylase activities, *J. Cell. Biochem. 93*, 57−67.
14. Barnes, P. J., Adcock, I. M., and Ito, K. (2005) Histone acetylation and deacetylation: importance in inflammatory lung diseases, *Eur. Respir. J. 25*, 552−563.
15. Van den Wyngaert, I., de Vries, W., Kremer, A., Neefs, J. M., Verhasselt, P., Luyten, W., and Kass, S. U. (2000) Cloning and characterization of human histone deacetylase 8, *FEBS Lett. 478*, 77−83.
16. Vannini, A., Volpari, C., Filocamo, G., Casavola, E. C., Brunetti, M., Renzoni, D., Chakravarty, P., Paolini, C., De Francesco, R., Gallinari, P., Steinkuhler, C., and Di Marco, S. (2004) Crystal structure of a eukaryotic zinc-dependent histone deacetylase, human HDAC8, complexed with a hydroxamic acid inhibitor, *Proc. Natl. Acad. Sci. U.S.A. 101*, 15064−15069.
17. Finnin, M. S., Donigian, J. R., Cohen, A., Richon, V. M., Rifkind, R. A., Marks, P. A., Breslow, R., and Pavletich, N. P. (1999) Structures of a histone deacetylase homologue bound to the TSA and SAHA inhibitors, *Nature 401*, 188−193.
18. Kadosh, D., and Struhl, K. (1998) Histone deacetylase activity of Rpd3 is important for transcriptional repression in vivo, *Genes Dev. 12*, 797−805.
19. Hassig, C. A., Tong, J. K., Fleischer, T. C., Owa, T., Grable, P. G., Ayer, D. E., and Schreiber, S. L. (1998) A role for histone deacetylase activity in HDAC1-mediated transcriptional repression, *Proc. Natl. Acad. Sci. U.S.A. 95*, 3519−3524.
20. Somoza, J. R., Skene, R. J., Katz, B. A., Mol, C., Ho, J. D., Jennings, A. J., Luong, C., Arvai, A., Buggy, J. J., Chi, E., Tang, J., Sang, B. C., Verner, E., Wynands, R., Leahy, E. M., Dougan, D. R., Snell, G., Navre, M., Knuth, M. W., Swanson, R. V., McRee, D. E., and Tari, L. W. (2004) Structural snapshots of human HDAC8 provide insights into the class I histone deacetylases, *Structure (Cambridge, MA, U.S.) 12*, 1325−1334.
21. Hernick, M., and Fierke, C. A. (2005) Zinc hydrolases: the mechanisms of zinc-dependent deacetylases, *Arch. Biochem. Biophys. 433*, 71−84.
22. Hernick, M., Gennadios, H. A., Whittington, D. A., Rusche, K. M., Christianson, D. W., and Fierke, C. A. (2005) UDP-3-O−(R-3-hydroxymyristoyl)-*N*-acetylglucosamine deacetylase functions through a general acid−base catalyst pair mechanism, *J. Biol. Chem. 280*, 16969−16978.
23. Auld, D. S. (2001) Zinc coordination sphere in biochemical zinc sites, *BioMetals 14*, 271−313.
24. Hildmann, C., Ninkovic, M., Dietrich, R., Wegener, D., Riester, D., Zimmermann, T., Birch, O. M., Bernegger, C., Loidl, P., and Schwienhorst, A. (2004) A new amidohydrolase from Bordetella or Alcaligenes strain FB188 with similarities to histone deacetylases, *J. Bacteriol. 186*, 2328−2339.
25. Sakurada, K., Ohta, T., Fujishiro, K., Hasegawa, M., and Aisaka, K. (1996) Acetylpolyamine amidohydrolase from Mycoplana ramosa: Gene cloning and characterization of the metal-substituted enzyme, *J. Bacteriol. 178*, 5781−5786.
26. Hu, E., Chen, Z. X., Fredrickson, T., Zhu, Y., Kirkpatrick, R., Zhang, G. F., Johanson, K., Sung, C. M., Liu, R. G., and Winkler, J. (2000) Cloning and characterization of a novel human. Class I histone deacetylase that functions as a transcription repressor, *J. Biol. Chem. 275*, 15254−15264.
27. Alonso, W. R., and Nelson, D. A. (1986) A novel yeast histone deacetylase - partial characterization and development of an activity assay, *Biochim. Biophys. Acta 866*, 161−169.
28. Johnson, C. A., Barlow, A. L., and Turner, B. M. (1998) Molecular cloning of Drosophila melanogaster cDNAs that encode a novel histone deacetylase dHDAC3, *Gene 221*, 127−134.
29. Fabiane, S. M., Sohi, M. K., Wan, T., Payne, D. J., Bateson, J. H., Mitchell, T., and Sutton, B. J. (1998) Crystal structure of the zinc-dependent beta-lactamase from Bacillus cereus at 1.9 angstrom resolution: Binuclear active site with features of a mononuclear enzyme, *Biochemistry 37*, 12404−12411.
30. Kanyo, Z. F., Scolnick, L. R., Ash, D. E., and Christianson, D. W. (1996) Structure of a unique binuclear manganese cluster in arginase, *Nature 383*, 554−557.
31. Rajagopalan, P. T. R., Yu, X. C., and Pei, D. (1997) Peptide deformylase: A new type of mononuclear iron protein, *J. Am. Chem. Soc. 119*, 12418−12419.
32. Zhu, J. G., Dizin, E., Hu, X. B., Wavreille, A. S., Park, J., and Pei, D. H. (2003) S-ribosylhomocysteinase (LuxS) is a mononuclear iron protein, *Biochemistry 42*, 4717−4726.
33. Tripp, B. C., Bell, C. B., Cruz, F., Krebs, C., and Ferry, J. G. (2004) A role for iron in an ancient carbonic anhydrase, *J. Biol. Chem. 279*, 6683−6687.
34. Parks, T. D., Howard, E. D., Wolpert, T. J., Arp, D. J., and Dougherty, W. G. (1995) Expression and purification of a recombinant tobacco etch virus NIa proteinase: biochemical analyses of the full-length and a naturally occurring truncated proteinase form, *Virology 210*, 194−201.
35. Gediya, L. K., Chopra, P., Purushottamachar, P., Maheshwari, N., and Njar, V. C. (2005) A new simple and high-yield synthesis of suberoylanilide hydroxamic acid and its inhibitory effect alone or in combination with retinoids on proliferation of human prostate cancer cells, *J. Med. Chem. 48*, 5047−5051.
36. Ling, M. M., and Robinson, B. H. (1997) Approaches to DNA mutagenesis: an overview, *Anal. Biochem. 254*, 157−178.
37. Gill, S. C., and von Hippel, P. H. (1989) Calculation of protein extinction coefficients from amino-acid sequence data, *Anal. Biochem. 182*, 319−326.
38. Smith, P. K., Krohn, R. I., Hermanson, G. T., Mallia, A. K., Gartner, F. H., Provenzano, M. D., Fujimoto, E. K., Goeke, N. M., Olson, B. J., and Klenk, D. C. (1985) Measurement of protein using bicinchoninic acid, *Anal. Biochem. 150*, 76−85.
39. Riddles, P. W., Blakeley, R. L., and Zerner, B. (1979) Ellman's reagent: 5,5'-dithiobis(2-nitrobenzoic acid)- -a reexamination, *Anal. Biochem. 94*, 75−81.
40. McCall, K. A., and Fierke, C. A. (2004) Probing determinants of the metal ion selectivity in carbonic anhydrase using mutagenesis, *Biochemistry 43*, 3979−3986.
41. D'Souza, V. M., Bennett, B., Copik, A. J., and Holz, R. C. (2000) Divalent metal binding properties of the methionyl aminopeptidase from Escherichia coli, *Biochemistry 39*, 3817−3826.
42. Porter, D. J. (2000) Escherichia coli cytosine deaminase: the kinetics and thermodynamics for binding of cytosine to the apoenzyme and the Zn(2+) holoenzyme are similar, *Biochim. Biophys. Acta 1476*, 239−252.

43. Jackman, J. E., Raetz, C. R., and Fierke, C. A. (1999) UDP-3-O-(*R*-3-hydroxymyristoyl)-*N*-acetylglucosamine deacetylase of Escherichia coli is a zinc metalloenzyme, *Biochemistry 38*, 1902−1911.
44. Schultz, B. E., Misialek, S., Wu, J., Tang, J., Conn, M. T., Tahilramani, R., and Wong, L. (2004) Kinetics and comparative reactivity of human class I and class IIb histone deacetylases, *Biochemistry 43*, 11083−11091.
45. Braun, V. (2003) Iron uptake by Escherichia coli, *Front. Biosci. 8*, s1409−s1421.
46. Larsen, K. S., and Auld, D. S. (1989) Carboxypeptidase-A-mechanism of zinc inhibition, *Biochemistry 28*, 9620−9625.
47. Bukrinsky, J. T., Bjerrum, M. J., and Kadziola, A. (1998) Native carboxypeptidase A in a new crystal environment reveals a different conformation of the important tyrosine 248, *Biochemistry 37*, 16555−16564.
48. Whittington, D. A., Rusche, K. M., Shin, H., Fierke, C. A., and Christianson, D. W. (2003) Crystal structure of LpxC, a zinc-dependent deacetylase essential for endotoxin biosynthesis, *Proc. Natl. Acad. Sci. U.S.A. 100*, 8146−8150.
49. Maret, W., Jacob, C., Vallee, B. L., and Fischer, E. H. (1999) Inhibitory sites in enzymes: zinc removal and reactivation by thionein, *Proc. Natl. Acad. Sci. U.S.A. 96*, 1936−1940.
50. Fersht, A. (1998) *Structure and Mechanism in Protein Science: A Guide to Enzyme Catalysis and Protein Folding*, pp 166, W. H. Freeman, New York.
51. Buggy, J. J., Sideris, M. L., Mak, P., Lorimer, D. D., McIntosh, B., and Clark, J. M. (2000) Cloning and characterization of a novel human histone deacetylase, HDAC8, *Biochem. J. 350*, 199−205.
52. Lee, H., Rezai-Zadeh, N., and Seto, E. (2004) Negative regulation of histone deacetylase 8 activity by cyclic AMP-dependent protein kinase A, *Mol. Cell. Biol. 24*, 765−773.
53. Berg, J. M., and Merkle, D. L. (1989) On the metal ion specificity of "zinc finger" proteins, *J. Am. Chem. Soc. 111*, 3759−3761.
54. Kobayashi, M., and Shimizu, S. (1999) Cobalt proteins, *Eur. J. Biochem. 261*, 1−9.
55. D'Souza, V. M., and Holz, R. C. (1999) The methionyl aminopeptidase from Escherichia coli can function as an iron(II) enzyme, *Biochemistry 38*, 11079−11085.
56. Porter, D. J., and Austin, E. A. (1993) Cytosine deaminase. The roles of divalent metal ions in catalysis, *J. Biol. Chem. 268*, 24005−24011.
57. Seffernick, J. L., McTavish, H., Osborne, J. P., de Souza, M. L., Sadowsky, M. J., and Wackett, L. P. (2002) Atrazine chlorohydrolase from Pseudomonas sp. strain ADP is a metalloenzyme, *Biochemistry 41*, 14430−14437.
58. Petrat, F., de Groot, H., Sustmann, R., and Rauen, U. (2002) The chelatable iron pool in living cells: A methodically defined quantity, *Biol. Chem. 383*, 489−502.
59. Outten, C. E., and O'Halloran, T. V. (2001) Femtomolar sensitivity of metalloregulatory proteins controlling zinc homeostasis, *Science 292*, 2488−2492.
60. Zeng, H., Bozym, R. A., Rosenthal, R. E., Fiskum, G., Cotto-Cumba, C., Westerberg, N., Fierke, C. A., Stoddard, A., Cramer, M. L., Frederickson, C. J., and Thompson, R. (2005) In situ measurement of free zinc in an ischemia model and cell culture using a ratiometric fluorescence-based biosensor, *Proc. SPIE-Int. Soc. Opt. Eng. 5692*, 51−59.
61. Keyer, K., and Imlay, J. A. (1996) Superoxide accelerates DNA damage by elevating free-iron levels, *Proc. Natl. Acad. Sci. U.S.A. 93*, 13635−13640.
62. O'Neill, H. A., Gakh, O., Park, S., Cui, J., Mooney, S. M., Sampson, M., Ferreira, G. C., and Isaya, G. (2005) Assembly of human frataxin is a mechanism for detoxifying redox-active iron, *Biochemistry 44*, 537−545.
63. Luk, E., Jensen, L. T., and Culotta, V. C. (2003) The many highways for intracellular trafficking of metals, *J. Biol. Inorg. Chem. 8*, 803−809.
64. Kelly, W. K., and Marks, P. A. (2005) Drug insight: Histone deacetylase inhibitors-development of the new targeted anticancer agent suberoylanilide hydroxamic acid, *Nat. Clin. Pract. Oncol. 2*, 150−157.
65. Li, J. Y., Chen, L. L., Cui, Y. M., Luo, Q. L., Li, J., Nan, F. J., and Ye, Q. Z. (2003) Specificity for inhibitors of metal-substituted methionine aminopeptidase, *Biochem. Biophys. Res. Commun. 307*, 172−179.
66. Namgaladze, D., Hofer, H. W., and Ullrich, V. (2002) Redox control of calcineurin by targeting the binuclear Fe(2+)-Zn(2+) center at the enzyme active site, *J. Biol. Chem. 277*, 5962−5969.
67. Ito, K., Hanazawa, T., Tomita, K., Barnes, P. J., and Adcock, I. M. (2004) Oxidative stress reduces histone deacetylase 2 activity and enhances IL-8 gene expression: role of tyrosine nitration, *Biochem. Biophys. Res. Commun. 315*, 240−245.
68. Fulco, M., Schiltz, R. L., Iezzi, S., King, M. T., Zhao, P., Kashiwaya, Y., Hoffman, E., Veech, R. L., and Sartorelli, V. (2003) Sir2 regulates skeletal muscle differentiation as a potential sensor of the redox state, *Mol. Cell. 12*, 51−62.

BI060212U